JOURNAL OF INNOVATIVE TRANSPORTATION

Progressive failure analysis of partially pre-stressed concrete railway sleepers

Ferhat Çeçen[a] iD, Bekir Aktaş[b,*] iD

[a] TCDD (Turkish State Railways), Concrete Sleeper Factory, Sivas, Turkey ✉
[b] Erciyes University, Civil Engineering Department, Kayseri, Turkey ✉

Highlights

- 50% more compression stress occurs in the A-type sleepers compared to N-type
- Frr value in more detail concerning the concrete tensile strength
- 25% higher stresses occur in A-type design than N-type design under Fr0.05 load

Abstract

Billions of sleepers are used on railways around the world today. As the importance of railways in the transportation sector is increasing, the demand for sleepers is also increasing. Although wooden and steel sleepers were used in rail systems in the past, today the most widely used sleeper type in the world is reinforced concrete sleepers. Among these reinforced concrete sleepers, pre-stressed sleepers are the most widely used, popular type of sleeper that can be produced in many countries. The two main production methods of pre-stressed sleepers are the ribbed reinforced system and the non-ribbed reinforced anchor plated system. In this study, B70 type pre-stressed concrete sleepers, have been investigated with the positive moment determination tests at the rail seat with progressive failure observations according to EN 13230-2:2016 standard. After tests, detailed cracking, failure, and fatigue analyzes under increasing test loads were performed with ANSYS® finite element analysis results for both types of pre-stressed sleepers. According to results, A-type sleepers have 50% more compression stress at the first crack formation load (Frr) than N-type sleepers and According to the first 0.05 mm permanent crack formation load (Fr0.05), it is seen that 25% higher stresses occur in A-type design than N-type design under Fr0.05 load. The results obtained through the analysis have been compared with the actual field measurement results, which have become more and more popular in the world in recent years. In this direction, various suggestions have been made for the development of concrete railway sleeper models.

1. Introduction

The components of classical ballasted railways are categorized as superstructure and infrastructure. As shown in Figure 1, while the rails and the sleepers are "superstructure" components; the ballast and the formation layer are "infrastructure" components. Sleepers are of great importance in protecting the road geometry and transferring the loads and vibrations taken from the rails to the infrastructure by damping [1]. Although wooden and steel sleepers were used in rail systems in the past, today the most widely used sleeper type in the world is the reinforced concrete sleeper. Among the reinforced concrete sleepers, pre-stressed reinforced concrete sleepers are the most widely used, popular type of sleeper that can be produced in many countries shown in Figure 1 [2].

Figure 1. Representation of conventional ballasted railway components

---

In Figure 2, the most widely used production methods of these pre-stressed reinforced concrete sleepers in the world are presented. With the long-line production process as shown in Figure 2.a, pre-stressed main-line sleepers and turnout bearers can be produced in the desired cross-section and length, including rectangular sections. Mold plates and accessories used in this process are easily available. As can be seen in Figure 2.a; High-capacity pre-stressing equipment is needed to keep the pre-stressing force strong along the tens of meters long production line. Produced concrete blocks, depending on the factory capacity, are cut in desired intermediate lengths. Therefore, it is practical to produce turnout bearer sets containing different lengths of sleepers. In this process, HTS (high tensile strength) class pre-stressing strands (tendons) are used, which can be obtained easily and at a low cost in the market. In addition to the ease of supply, these strands are self-ribbed and do not require a special process, anchoring equipment, or labor for their use, providing significant advantages in sleeper production cost.

The carousel process is given in Figure 2.b requires high automation. In this process, a cyclic process is carried out in the form of "cleaning of sleeper molds-assembly of connection materials-pre-processing-concrete placement - rotating disassembly-cleaning of sleeper molds". In this system, steel molds are usually used that serve to produce 2 or 4 sleepers together and are strong enough to meet the pre-stress force. In this way, 2-4 sleepers in each cycle are prepared for the curing process. In this process, the used molds bear the pre-tensioning force until the concrete is cured, so sleeper molds are needed for about 14 hours production process. Unlike the long line process, the HTS rods in this process must be subjected to special workmanship such as screw-cutting, bending, mounting the anchor plates, etc. depending on sleeper sizes and production process. With the carousel system, the pre-stressed sleepers can be produced with pre-tensioned or post-tensioned processes. But the carousel system is not feasible for turnout bearers since the connection material positions and sleeper lengths of the turnout bearers vary greatly. According to the results of the tests performed on the sleepers with various reinforcement and anchorage structures given in Figure 3; It is stated that the ultimate strength of sleepers in fatigue tests is higher with the use of anchored and/or a larger number of reinforcements usage [3]. Pre-stressed sleepers can be produced differently from these systems and even with various reinforcement numbers or anchorage processes. More reinforcement number usage has a bigger bonding surface, also ribbed surface produces smaller or no anchor plate usage. A bigger anchor surface produces smaller early concrete strength and longer fatigue life.

Figure 2. Common production methods of pre-stressed reinforced concrete sleepers: a. Pre-stressed sleeper production with long-line system b. Pre-stressed sleeper production with a carousel system

Figure 3. Various reinforcement and anchorage mechanisms in carousel sleeper production system a. Without ribbed-with anchor plate, b. Ribbed-with anchor plate, c. Ribbed-without anchor plate [3]

In pre-stressed sleepers, the reason for applying the pre-stress is to prevent or limit bending cracks in service [4]. As it is known, tensile stresses occur in structural elements under simple bending. Since the tensile strength of concrete materials is low to be neglected, steel-reinforced concrete structures have been developed. In reinforced concrete elements, the concrete material needs to be deformed to meet the tensile stresses by engaging the reinforcements, and cracks are inevitable when the deformation level in the concrete increases. In pre-stressed designs, before the service loads affect the structural element, pre-stressing compression is provided to the element over the reinforcements. This pre-compression capacity eliminates the tensile stresses "partially" or "completely" [1]. The phrases "partially" and "completely" in this definition make great differences in terms of product performance. Early pre-stressed concrete designers focused on eliminating tensile stresses in structural members. This design method is called a "fully pre-stressed" system. However, loads above the calculated design load may occur in the elements that cannot be fully predicted (such as railway sleepers). Also, it is quite complicated to predict whether tensile stress occurs in the concrete section, depending on the distribution variability of the minimum and maximum moment occurring along the cross-section. Therefore, either complex and expensive sections are used or the pre-stressing force is increased to stay in the safe zone [5]. As the experience of pre-stressed systems increases, it has been seen that the elements to be designed between the classical non-pre-stressed system and the fully pre-stressed system offer many advantages. These systems, where tensile stresses in concrete are allowed at a specified level under full-service load, are called "partially pre-stressed" designs. With this method, a more economical design can be applied with smaller cross-sectional areas and less reinforcement can be used. Also,

under ultimate load, partially pre-stressed systems show higher ductility than fully pre-stressed systems and can absorb more energy against high dynamic loads such as earthquakes or explosions [6].

Today, the partially pre-stressing design philosophy explained above is applied in pre-stressed railway sleepers. In the pre-stressed railway sleepers, as long as the train does not affect the road, there is a pre-stressing compression continuously acting towards the sleeper center. Thanks to this additional capacity, no cracks occur in the sleeper (invisible because tensile stresses occur, but it does not exceed the crack resistance) up to the fatigue design load (Fr0). While the train is affecting the road, this compression decreases repeatedly towards zero and if the impact load is more than the pre-stressing capacity (decompression load), it starts to increase as a negative (tensile stress) [1]. Despite the advantages mentioned above, partially pre-stressed members reaching their fatigue limit under repetitive reversible loads can be a cause for concern. Cracks are formed in the partially pre-stressed elements under the effect of the first dynamic loads, and in the following dynamic loads, cracks with a lower value than the first appear again. Although it is predicted that in fully pre-stressed uncracked sections, the pre-stressing force (due to the stretching of the concrete, relaxation of the reinforcement, etc.) will decrease by approximately 14%, this value is quite high in the cracked sections [6]. For these reasons, sleepers produced with the partially pre-stressing process are not desired to be exposed to loads higher than the fatigue design load (Fr0), and according to standards such as EN 13230-1 / 2 on railway sleepers, loads above this limit are called exceptional (Fr0.05), so that a very small number of them allowed in the service life [7]. Because under these repetitive reversible loads, early fatigue and higher capacity losses are seen [1].

In the literature, there are many studies on the comparison of the impact loads on the railway with the pre-stressing capacity of the sleepers, and also on the insufficiency of the capacity of the existing sleepers, a sample study is presented in Figure 4 [8]. When trainloads affect the partially pre-stressed railway sleepers, the pre-stressing capacity is reached first (decompression), then the first cracks become visible after a little more load is carried due to the cracking resistance of the concrete section (Frr). As can be seen from Figure 4, before the cracking load of the partially pre-stressed sleepers starts, the pre-stressing capacity is used up and the "decompression" load is exceeded. After this load value, firstly elastic and then plastic deformations are observed in concrete and reinforcement. Also, as can be seen from Figure 4, the record of the loads exceeding the pre-stressing capacity is quite higher than the allowed capacity of standards, and even in the short period of 12 months, the number of loads exceeding the cracking load reaches tens of thousands. Like this study, various field measurement studies have been carried out on railways

in recent years and the adequacy of the sleeper design loads calculated with empirical approaches in the past has been questioned. Indeed, it will not be fully correct to compare field record peak values with the static and fatigue test results of existing sleepers. Because the characteristics of the real railway conditions such as strain rate, load duration, and support conditions are greatly different from the tests in question. On the other hand, depending on the railway operating capacity, the number of load repetitions is also quite high, and there are different effects in different parts of the sections and continuous changes in the forced sections. So, the service life is highly predicted to decrease under these high magnitude impact loads. Meanwhile, the real cracking mechanics of the railway sleepers need to be examined in more detail with special analysis methods that include the real load characteristics of railways.
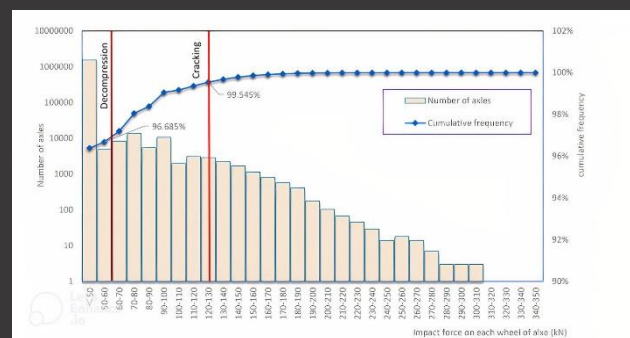

Figure 4. The cumulative frequency of the load values that create decompression and crack initiation in sleepers according to railway field measurement records [8]

The applied partially pre-stressing compression to the sleepers and the use of corrosive steel reinforcements bring many disadvantages, even in the most modern designs. For this reason, cracks that progress gradually (and completely or partially closed with the effect of pre-stressing force after the train passes) cannot be prevented in the sleepers. With the effect of these cracks, the concrete is damaged and the pre-stress force decreases, and the chlorine ions penetrating the concrete cause corrosion in the pre-stressing steel. Therefore, sleeper life ends before the planned (40/50-year) service life [9]. While corrosion can occur even when there is no crack in reinforced concrete structures, it becomes easier to occur with the formation of cracks. And it's well known that a material's corrosion susceptibility changes significantly after being pre-stressed or bent, and cyclic loading of a material accelerates stress-induced corrosion cracking. Also, the diameter of the used reinforcement for pre-stressing is smaller than the conventional system. For this reason, a small amount of local corrosion or a thin layer of corrosion causes a significant decrease in the reinforcement cross-sectional area and consequently, it breaks [6]. There are various studies in the literature on corrosion damages occurring in pre-stressed railway sleepers [10].

In this study, B70 type pre-stressed concrete railway sleepers, have been investigated with the positive moment determination tests at the rail seat with progressive failure observations according to EN 13230-2:2016 standard. After tests, detailed cracking, failure, and fatigue analyzes under increasing test loads were performed with ANSYS® finite element analysis results for both types of pre-stressed sleepers. The results obtained through the analysis have been compared with the actual field measurement results, which have become more and more popular in the world in recent years. In this direction, various suggestions have been made for the development of the concrete railway sleeper models.

2. Material and Method

2.1. B70 type railway sleepers and positive moment determination test procedure

The descriptive codes of the reinforced concrete sleepers developed and expanded in Germany contain a number after the letter B. The letter B stands for concrete and the number after the letter represents the design year of the sleeper [11]. The curing process of manufactured B70 type sleepers and fresh concrete samples was carried out following EN 13230-1:2016. After the curing period of 28 days, the sleepers were subjected to the "static positive moment determination tests at the rail seat", which is given the test setup and loading procedure in Figure 5 per EN 13230-2:2016. In this standard, the conditions of static loading positive moment determination test on the rail seat to be applied in the acceptance and design of pre-stressed sleepers are given [7]. In the test phase, the support distance is 60 cm. Loading is carried out until the first crack is detected (Frr) or up to the load value determined by the railway establishment (Fr0). Then, the load is increased by 10 kN and kept constant for 10 seconds to 5 minutes, then the load is removed and the crack is checked with a lens. In this way, when the load is removed with 10 kN increments, if a plastic crack above a thickness of 0.05 mm is detected, the second recording data (Fr0.05) of the experiment is found. Finally, by continuing the loading-unloading procedure, the breaking load (FrB) is recorded, where the section cannot carry more load [12].

2.2. Finite element modelling for cracking mechanics analysis

ANSYS® 2020 R1 software, which is widely used worldwide, was used in the finite element analysis conducted within the scope of this study. In sleeper modeling, only half of the whole body affected by the test supports was modeled using the "symmetry" feature in the ANSYS Mechanical module, and thus analyzes was easily performed. In concrete material modeling, "Concrete NL" material from the "non-linear engineering materials" in the material library and the Drucker-Prager model from the "GeoMechanical" material models in the

toolbox menu were used. In finite element analysis, 3 methods are widely used in modeling the reinforcement. These are the assumption of smeared reinforcement based on the reinforcement cross-section ratio, the embedded reinforcement assumption, where the reinforcement is assumed as axle elements combined with concrete, and the discrete reinforcement assumptions made up of completely separate elements. In this study, apart from these three models, separate modeling, which provides a more detailed analysis, was applied as shown in Figure 6. Thanks to this model, is better than the discrete reinforcement assumption, which is shown as the most effective of the common reinforcement models; Instead of one-dimensional "truss" elements, three-dimensional "solid" elements were used and all the loads that the reinforcement would be subjected to were taken into account. As can be seen in Figure 6, in the finite element analysis, two different production methods with ribbed-reinforced and plane reinforced-anchor plated sleeper types are modeled and detailed stress and deformation characteristics are analyzed mutually. The issue of mesh overlap, which is of great importance in reinforcement modeling in a ribbed design, is provided with the shared topology option in the SpaceClaim® software that comes with the ANSYS program. For the anchor-plated model, frictionless contact modeling was applied without sharing the topology between the reinforcements and concrete, and full adherence was applied by modeling "bonded contact" only on the reinforcement-anchor plates-concrete contact surfaces.
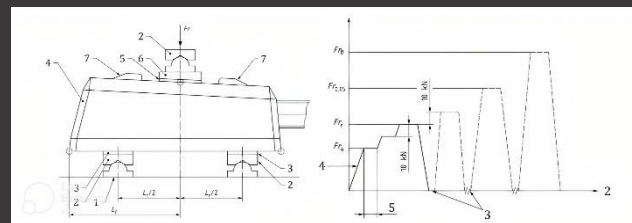

Figure 5. Test setup (left) and static test procedure (right) (left figure; 1: rigid support, 2: articulated support, 3: resilient pad, 4: sleeper, 5: standard rail pad, 6: tapered packing, 7: lateral stop and base plate (figure on the right; 1: load, 2: time, 3: crack control, 4: loading speed limit 120 kN / min, 5: standby time (10 seconds-5 minutes)) [7]

To create stress-strain curves for HTS class steel reinforcement, the yield strength values of 1585 MPa and tangent modulus 2628 MPa were entered in the "bi-linear" material properties section of the Structural Steel NL material in the ANSYS material library. In the modeling of the pre-stressing force, the "inistate" command of ANSYS software was used. Before the test load is affected, a separate "load-step" is created and pre-deformation is given in the direction of the reinforcement axis. In the tested B70 type sleepers, 4 pieces of HTS class steel reinforcement with a diameter of 9.4 mm were used. Approximately 75.53 Newton pre-stress force is applied to these rods, and approximately 1090 MPa pre-stress compression is provided in each reinforcement. ANSYS

Solid 186 and Solid 187 element types were preferred for modeling both concrete elements and reinforcements. These high-quality elements have 3 dimensional, 20 points, and quadratic deformation capability and are recommended for detailed analysis. These 20 separate points have freedom in 3 axes and offer advantages of plasticity, hyper elasticity, creep, large deflections, pre-stressed design, and layered composite modeling [13]. To fully obtain the advantages specified from Solid 186-187 elements and to avoid convergence problems, a "hex-dominant" (hexagonal) mesh configuration was applied as suggested in the literature and shown in Figure 6 [14]. Finite element mesh sizes have a significant effect on higher or lower stress results. The use of a smaller mesh size reduces the energy distribution, so it can show the breaking load less than it is, however, the use of a bigger mesh size can show the breaking load higher than it is because it reduces the crack development [15]. After the mesh operation is done, the evaluation criteria should be accessed under the "mesh metric" line in the "statistics" section. At this stage, the "skewness criterion" is the most widely used and valid. A skewness value up to 0.94 can be accepted, but if it is above this, a poor-quality mesh can be mentioned [16]. In analyzes, the mesh quality was calculated by ANSYS as 0.686 for the ribbed design and as 0.234 for the un-ribbed design in terms of "skewness", and analyzes were continued, seeing that they are of sufficient quality. The higher mesh quality of the un-ribbed design is due to the lack of reinforcement-concrete topology sharing.
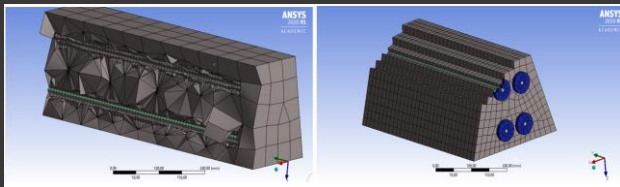

Figure 6. Finite element mesh modeling of two different pre-stressed sleeper types; ribbed-reinforced type (left) and plane reinforced-anchor plated type (right)

It is of great importance to define the support conditions correctly during the sleeper tests to obtain an accurate and unique solution. In EN 13230-2 tests, the bearings have a rectangular contact surface that can rotate in the bending direction, with a width of 10 cm, and also plastic interfaces are used to reduce local crushes [7]. In this context, simulation analyzes were carried out for various support conditions. It was observed that the more accurate support condition, which gives the same results as the applied experiments, is "remote displacement" supports of 10 cm width that allow horizontal (UY) movement and rotation in the X-axis on both supports. Also, it was decided to apply a "remote force" condition in which only vertical (UZ) movement is allowed on the rail support with the hydraulic press loading assembly and "deformable" interfaces instead of "rigid" intermediate elements in all three interfaces. As given in Figure 7; In both remote displacement and remote force applications, contact surfaces are modeled not in the "line" form,

which is frequently encountered in practice, but real area (surface) definitions of 10 cm width are made and more realistic results are obtained. To obtain detailed results with non-linear modeling during analyzes, the "large deflections" setting was turned on in the analysis settings. Also, to prevent convergence error, the applied load is increased not in one step, but in 20 stages (load steps), and these stages are divided for the second time with a minimum of 3 "sub steps". In this way, the stiffness matrix in each stage is updated before moving to the next load stage [17]. During analyzes, the non-linear Full Newton-Raphson iteration procedure and automatic time stepping were set, allowing the stiffness matrix to be updated at each iteration. After all these adjustments, the solution time of the software has increased considerably. However, in this way, ANSYS software was able to predict and control the new loading steps based on the past solution records and advance the load steps per the accuracy of the convergence graph.
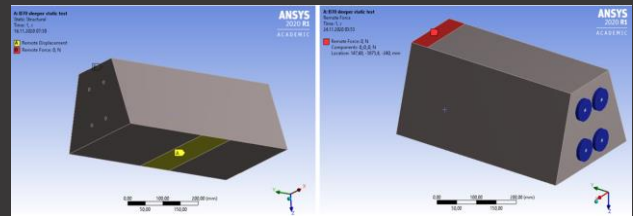

Figure 7. Modeling of support and loading conditions of static test setup in accordance with EN 13230-2.

3. Findings

3.1. Experimental test results

During the sleeper production, 150x150x150 mm cube and 150x300 mm cylinder samples were taken from the pre-stressed reinforced concrete sleepers, and compression and splitting tensile tests were performed. Test results and used other parameters in ANSYS finite element analyzes are presented in Table 1. The compressive strength result of concrete was determined 68.0 MPa which is C50 / 60 class in accordance with the TS EN 206-1 standard [18]. So, in finite element analyzes, the 50 MPa value was entered as characteristic compressive strength. According to the test results given in Table 1 and TS 500: February 2000 equation 3.2, the elasticity module of the concrete was calculated as 36981 MPa [19]. The characteristic splitting tensile strength of concrete was calculated as 4.16 MPa in accordance with TS EN 206-1 standard from the splitting tensile test results with an average value of 4.66 MPa and the direct (uniaxial) tensile strength is calculated as 2.77 MPa by dividing this value by 1.5 [19]. The Poisson's ratio is equal to a constant value as long as the strains remain within elastic limits. This value is approximately 0.15 - 0.20 for concrete [20]. In the literature, there are studies on the use of a 0.25 value for beam elements under bending [17]. The Poisson's ratio of concrete has an important effect on the correct calculation of the reinforcement stresses, and

in this study, the average value of 0.25 was used considering the bending load of the sleepers during the tests and the lower trapezoidal sleeper section dimensions. Obtained load value-crack thickness measurements with lens and crack width gauge after each loading step are presented in Table 2 and sample test visuals are presented in Figure 8-Figure 12. The crack development mechanism in the figures is shown in blue for cracks that are closed after the load is removed, and in red if a permanent crack of 0.05 mm or more remains after the load is removed. As can be seen; the first crack observation (Frr) in sleepers occurred in the 190-210 kN range. After the loads at this level are removed, the cracks close again with the effect of the pre-stressing compression. The first crack formation load value is important in proving the adequacy of the pre-stressing compression in pre-stressed sleepers, and it is routinely checked with random samples taken from the daily production of factories. The next part of the test is referred to as "design approval tests" and does not require routine control without process changes [7]. The second design parameter requested in EN 13230-2 is the load value at which a 0.05 mm permanent (plastic) crack occurs (Fr0.05), and the last parameter is the breaking load (FrB), as can be seen in Figure 5 [7].

Table 1. Cube and cylinder concrete test results and finite element model parameters

Concrete parameters	Results
Compressive strength test result (average)	68,0 MPa
Concrete compressive strength class (EN 206-1)	C50/60
Concrete characteristic compressive strength (fck)	50 MPa
Initial elasticity modulus of concrete (TS 500)	36981 MPa
Poisson's ratio of concrete (from literature [17])	0,25
Splitting tensile strength test result (average)	4,66 MPa
Characteristic tensile strength (EN 206-1)	2,77

Figure 8. First crack formation (Frr = 190 kN) and permanent crack load (Fr0.05=300 kN) after the test load is removed

Figure 9. Cracks occurred at the first crack formation load (Fr$_r$ = 210 kN) and permanent crack load (Fr$_{0.05}$=290 kN) after the test load is removed

Table 2. EN 13230-2 Static loading positive moment determination test results at rail seat

Test / measurement parameters	Results (kN)
First crack formation (Frr)	205
First crack onset after 230 kN load	190
First crack onset after 240 kN load	160
First crack onset after 250 kN load	150
First crack onset after 260 kN load	130
First crack onset after 270 kN load	130
First crack onset after 350 kN load	70
First crack onset after 360 kN load	70
Permanent crack of 0.05 mm (Fr0,05)	288
Permanent crack of 0.20 mm	300
Permanent crack of 0.35 mm	330
Permanent crack of 0.50 mm (Fr0,5)	350

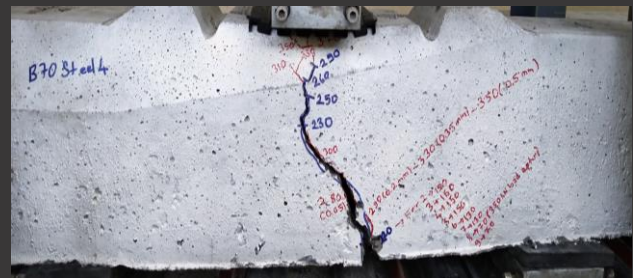Figure 10. Cracks occurring under 380 kN static load, while the test load continues to act

Figure 11. Permanent crack levels occurred under the effect of various test stages and the change in the first crack formation load under the effect of increasing loads
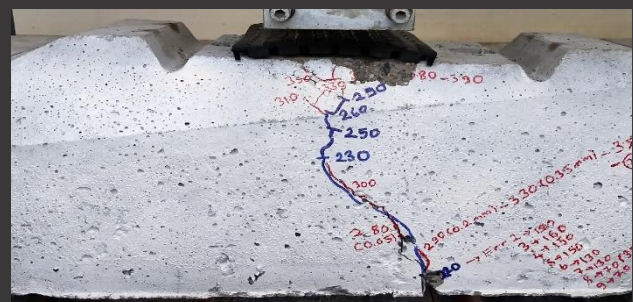

Figure 12. Cracks in the sleeper after 430 kN breaking load (Fr$_B$)

3.2. Finite element analysis results

Analyzes were performed on two major types of B70 sleepers. The first one is the sleeper containing ribbed reinforcements without an anchor plate and will be referred to as "N-type". The second type is an anchorage plated sleeper containing un-ribbed reinforcements and will be referred to as "A-type".

3.2.1. Stresses in concrete and reinforcement under the effect of pre-stressing force

The equivalent stress distribution in the concrete and reinforcements for the N-type sleeper under the effect of the pre-stressing force is shown in Figure 13. As is seen in this figure, approximately 1135 MPa equivalent tensile stress occurs in the reinforcement due to the pre-stressing force. This value coincides with the previously calculated 1090 MPa pre-stress strength for physical applications. Local stress concentrations are largely minimized since the topology is shared during the geometry arrangement. In finite element analyzes that require more detail, it is possible to completely prevent stress concentrations by making local mesh settings (refinement, etc.) of the mesh sizes at the contact locations of concrete and reinforcement. As is seen in Figure 13, after the pre-stressing process, while the compression stresses exceed 40 MPa near the concrete-reinforcement contact surface, this value decreases to approximately 7.2 MPa in the upper compression lobe and shows the minimum value at the bottom face because of the B70 type sleepers' trapezoidal cross-section. As can be seen from Figure 15, where the equivalent stress distribution for this location is given, there is only 5.7 MPa compressive stress at this location.
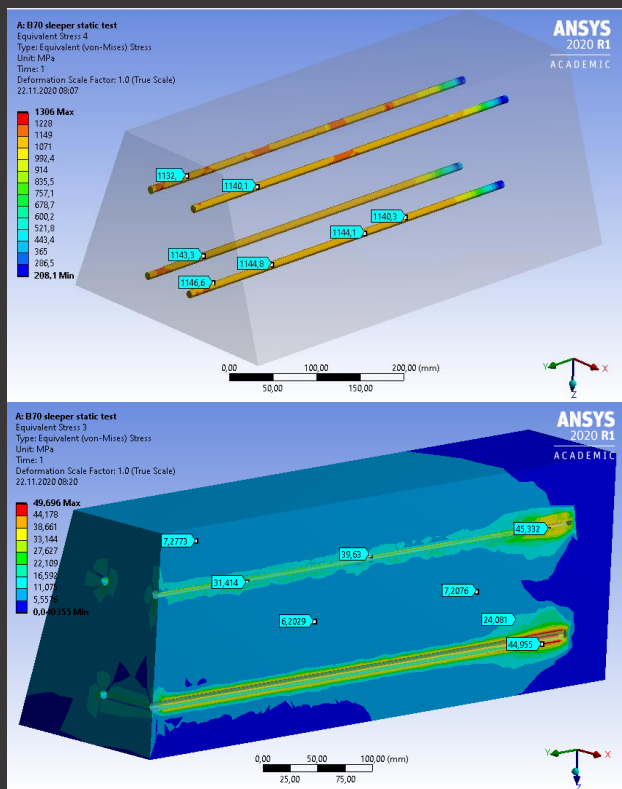

Figure 13. N-type sleeper equivalent stress (MPa) distributions of concrete and reinforcements after pre-stressing

The equivalent stress distribution in the concrete and reinforcements for the A-type sleeper under the effect of the pre-stressing force is shown in Figure 14. As is seen in this figure, approximately 1127 MPa equivalent tensile stress occurs in the reinforcement due to the pre-stressing force. This value coincides with the previously calculated 1090 MPa pre-stress strength for physical applications. As can be seen in Figure 14, the stresses seem higher than normal at some contact points where the reinforcement transfers load to the anchor plates. As stated before, in detailed finite element analyzes, it is possible to prevent stress concentrations with local mesh settings at contact locations. As is seen in Figure 14, after the pre-stressing process, while the compression stresses exceed 40 MPa near the anchor plate contact surface, this value decreases to approximately 7.5 MPa in the upper compression lobe and shows the minimum value at the bottom face because of the B70 type sleepers' trapezoidal cross-section. As can be seen from Figure 15, where the equivalent stress distribution for this location is given, there is only 5.2 MPa compressive stress at this location. Considering the yield strength (1350-1600 MPa) and fatigue limit (1200-1400 MPa) of the used HTS type reinforcements, for both N and A-type sleepers, the pre-stressing force is limited up to 75 kN (1100 MPa) for each of 4 reinforcements each with a cross-section of 69 mm^2. So, a total of approximately 320 kN pre-stressing force is obtained. However, a smaller number of reinforcement strands/rods or smaller anchor plates can cause higher stresses than the 20-35 MPa fatigue limit of sleeper concrete. The total circumference (reinforcement-concrete contact surface) of the 4 pieces of 9.4 mm diameter reinforcement in the analyzed sleepers is 118 mm. If the number of pieces is increased without decreasing the total reinforcement cross-section in sleeper production, for example, if 12 pieces of reinforcement with a diameter of 5.4 mm are used, the total circumference increases above 200 mm. In this case, the contact stresses that will occur in the concrete will decrease considerably, and the need for early high strength during production will also decrease. A similar approach is valid for the anchor plate geometry.

3.2.2. Determination of decompression load

After modeling the pre-stressing force, static loading positive moment test analysis at the sleeper rail seat was started. As the load acting at the rail seat increases, the pre-stress compression effects of the reinforcements gradually decrease and change direction at a certain point (decompression load value) theoretically beginning to work like typical non-stressed reinforced concrete structures. However, this is valid for the places near cracked areas, and different behaviors occur in different locations of the sleepers. The stress sensor is modeled at the bottom of the mid-span cross-section of the sleeper to determine the load value (decompression), where the pre-stressing force is finished and the reinforcements start to carry loads like non-pre-stressed designs and the resulting stress distributions are presented in Figure 15. As can be seen from this figure, the "compression" stress occurring in the concrete section under the effect of the pre-stressing gradually decreases with the effect of the test load acting on the sleeper rail seat. It starts to

increase as "tensile" stress, reaching the bottom point at a load value of about 82 kN in N-type and 76 kN in A-type.
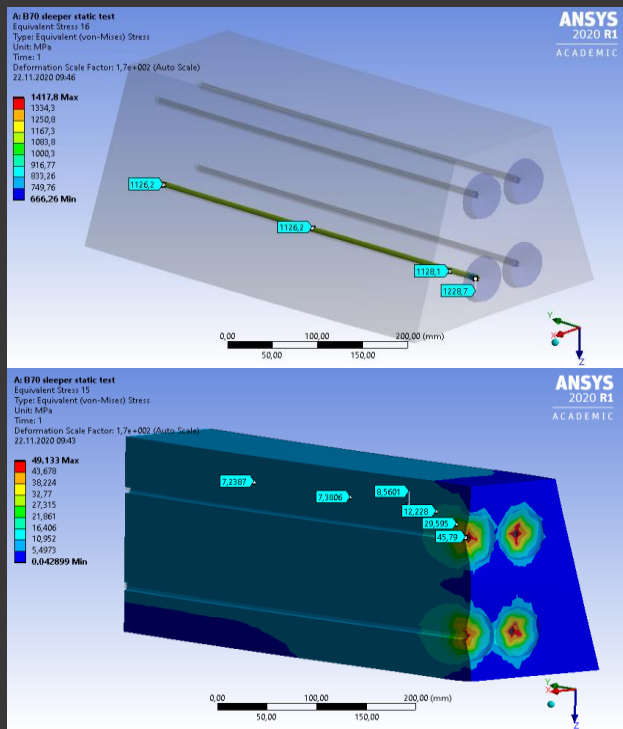

Figure 14. A-type sleeper equivalent stress (MPa) distributions of concrete and reinforcements after pre-stressing
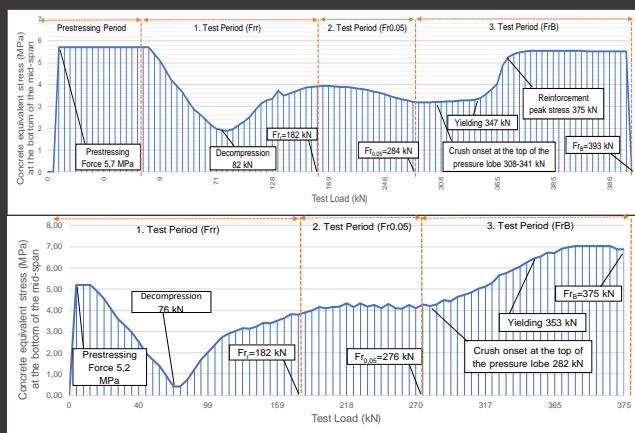

Figure 15. Concrete equivalent stress (MPa) at the bottom of the mid-span cross-section of the sleeper vs test load (kN) curves; up-side: N-type sleeper, down-side: A-type sleeper

The fatigue life of pre-stressed sleepers at loads under decompression capacity is considered to be "infinite" if a correct reinforcement and anchoring mechanism is applied. According to the recent field records given as an example in Figure 4, 96.685% of the loads affecting the sleepers are under the decompression capacity. In other words, it can be said that the sleepers will be subjected to an average of 300 million load repetitions during the targeted service life of 50 years, 290 million of them are within pre-stressing capacity.

3.2.3. Determination of first crack formation loads (Fr_r)

Experiments to detect cracks in pre-stressed sleepers can often be misleading. The reason for this is that the cracks remain at the micro level due to the effect of the pre-stressing compression. Therefore, in EN 13230-2, test loading speed is limited to 120 kN / min during the first crack detection and inspection with a lens that can magnify at least 20 times is required instead of naked-eye inspection [7]. Another point to be considered is, as specified in EN 13230-1; In the first crack formation detection, only the cracks "reaching a height of 15 mm from the sleeper bottom" should be recorded [7]. The first crack (Fr_r) observed in the laboratory tests was determined as 205 kN. In the finite element model, as can be seen from Figure 15, where the equivalent stress (MPa) distribution of the concrete material at the bottom of the mid-span cross-section of the sleeper is given, the first crack formation loads are determined as 182 kN in both the sleeper types. The reason why the early deformations are higher in N-type sleepers is that the reinforcement contact surfaces to which the pre-stressing force is transferred in N-type sleepers are much closer to the midsole point where the deformation sensor is located than the anchorage plates in A-type sleepers. The detected first crack formation loads were also confirmed and compared with Figure 16 where the maximum principal and equivalent stress distributions of concrete and reinforcements are given. In the maximum principal stress distributions locations that exceed the tensile strength of concrete of 2.77 MPa are shown with red fill. The determined values by finite element analyzes are slightly lower than the laboratory test results. This difference may have resulted from the sensitive crack formation process as stated above and the use of safety coefficients or with various assumptions in finite element analyzes. As can be seen from Figure 16, at the first crack formation load, 50% more compression stress occurs in the upper lobe of A-type sleepers compared to N-type sleepers. When the stress values of the reinforcement are examined, it is seen that there is approximately 10% more stress in the A-type sleepers, also the maximum value occurred near the anchor plates, unlike the "N-type". It can be also seen from the maximum principal stress distributions in Figure 16 that in N-type sleepers there are fewer cracks and less width. The service life of pre-stressed sleepers at loads above the decompression capacity begins to decrease due to fatigue. As before-mentioned, above the decompression capacity, the stresses in the pre-stressing reinforcement change direction (transforming). Today, fatigue tests with 3-5 Hz frequency and approximately 50-150 kN load cycles are performed in sleeper design approval tests. For example, according to EN 13230 standard, after 2 million loading cycles, a maximum loss of 45 kN in breaking load is anticipated for B70 type sleepers (from 375 kN to 330 kN). In case of operating conditions above the number and magnitude stipulated in the standard, this loss of capacity will increase even more. According to the recent field

records given as an example in Figure 4, 3.315% of the loads affecting the sleepers are above the decompression capacity. In other words, it can be said that the sleepers will be subjected to an average of 300 million load repetitions during the targeted service life of 50 years, and approximately 10 million of them are expected to remain above the decompression value. While high magnitude railway loads have a very high strain rate and their duration of action is quite short, depending on the railway operating capacity, the number of load repetitions is also quite high, and on the other hand, as can be seen from Figure 16, there are different effects in different parts of the sections and continuous changes in the forced sections. So, the service life begins to decrease due to fatigue.

In line with the analysis results presented so far, it can be easily inferred that the first crack capacity (Fr_r) consists of the combination of the pre-stressing capacity (decompression) and the tensile strength of the concrete. As given in Table 2, it has been determined by laboratory tests that the load value observed in the first crack formation load decreases from 206 kN to 130 kN after a few load repetitions within the elastic deformation limits of the reinforcement (210-277 kN). In the experiments conducted with non-pre-stressed sleepers produced with equivalent concrete and cross-section of B70 type pre-stressed sleepers, it was observed that the first crack formation could occur at a load of approximately 120 kN [1]. The combination of an average cracking strength of concrete of 120 kN and a decompression load of 76-82 kN coincides with the average first crack formation load of 206 kN obtained in laboratory tests. Concrete technology in the years when B70 and similar type sleepers were designed, has developed considerably today. Therefore, a revision of the first crack formation load test is required considering the tensile strength of today's high-performance concrete. As determined, the visible crack starting load value (Fr_r) in pre-stressed sleepers is the combination of pre-stressing capacity (decompression) and tensile strength of concrete. Today, the minimum value (Fr_0) of the first crack formation load that can be observed in B70 type pre-stressed reinforced concrete sleepers has been determined as 150 kN [12]. The cracking strength of concrete depends on many factors such as maximum aggregate diameter, granulometry, aggregate surface roughness, and placement quality and can give results in a wide range (50-150 kN). If concrete with a cracking resistance of 75 kN and above is used, it may not be fully controlled in routine controls whether the pre-stressing force is applied sufficiently or not. In other words, the first crack starting a load of 150 kN capacity or a big part of it can easily be reached in sleepers with high tensile strength of concrete, although not enough pre-stressing force is applied. In this respect, it is thought that it would be more appropriate to control the first crack formation load (Frr) value in more detail with the concrete tensile strength used in sleeper production.
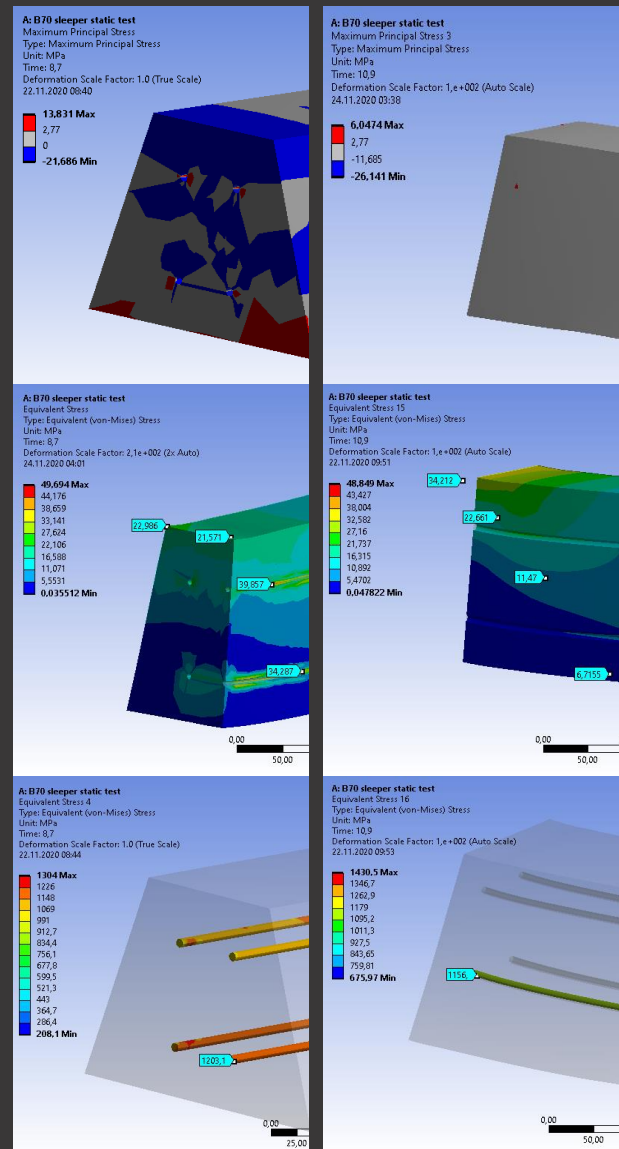

Figure 16. Comparative analysis results of concrete and reinforcements at Fr_r test loads in N-type sleeper (left-sides) and A-type sleeper (right-sides)

3.2.4. Determination of permanent crack loads ($Fr_{0.05}$)

Another parameter required in TS EN 13230-2 is the permanent crack ($Fr_{0.05}$) load of 0.05 mm thickness. Since cracks occurring up to this load value occur within elastic limits, it closes again with the effect of pre-stressing pressure after removing the load. According to laboratory tests, elastic cracks extend to the middle of the sleeper height at approximately 200-250 kN and the upper part of the compression lobe around 270-300 kN. At the same time (270-300 kN), cracks with a thickness of 0.05 mm ($Fr_{0.05}$) that do not fully close (plastic) when the load is removed are started to be detected at the bottom of the mid-span. In finite element analysis, the permanent crack formation loads are detected and compared with Figure 17 where the maximum principal and equivalent stress distributions of concrete and reinforcements are given. In the maximum principal stress distributions locations that exceed the tensile strength of concrete of 2.77 MPa are shown with red fill. Accordingly, the $Fr_{0.05}$ load was

determined as 282 kN in the N-type design and 276 kN in the A-type design. Obtained values significantly coincide with the physical test result of 288 kN. According to results, similar to the first crack formation load, the number, and width of the cracks are lesser but thicker at un-ribbed A-type design, as can be seen from maximum principal stress distributions. As regards concrete stresses, it is seen that 25% higher stresses occur in the A-type design than in the N-type design under the $Fr_{0.05}$ load. In the A-type design, it is seen that the ultimate strength of 50 MPa has begun to be exceeded both in the compression lobe and near the anchor plate. The occurrence of higher deformations has a great effect on the occurrence of this situation in the A-type design. In terms of reinforcement stresses, the stresses at the mid-span cross-section of the N-type sleepers and the stresses at the anchor plate location in the A-type sleepers gave similar results. As seen, the level of deformation occurring in A-type sleepers is much higher than in type N.

According to the results of the field measurements given in Figure 4, 99.545% of the loads to be placed on the sleepers are below the first crack formation load value. In other words, it can be estimated that the sleepers will be exposed to approximately 1.3 million loads above the first crack formation load value during the targeted 50-year service life. As can be seen from Figure 17, at the $Fr_{0.05}$ load level, stresses exceeding the fatigue limit occur in the reinforcement (1400-1500 MPa) and concrete (40-50 MPa) in both types of pre-stressed sleeper. An important point, while high magnitude railway loads have a very high strain rate and their duration of action is quite short, depending on the railway operating capacity, the number of load repetitions is also quite high, and also as can be seen from Figure 17, there are different effects in different parts of the sections and continuous changes in the forced sections. So, the service life begins to rapidly decrease due to fatigue, corrosion, and loss of pre-stress force. Under these repetitive reversible loads, early fatigue and higher capacity losses are seen [1]. As a result of laboratory experiments as can be seen in Figure 12, it was determined that the load value of first crack formation (Fr_r) starting in pre-stressed sleepers decreased up to 70 kN. Considering that sleepers are exposed to millions of load repetitions on railways, these capacity losses, determined by a few load repetitions, can be expected to occur at a higher level in actual field use. It is also stated in the FIB-CEB categorization; that it is recommended to apply "full pre-stressing" in structures that will be exposed to fatigue due to dynamic load or corrosive effects [5]. On the other hand, in the sleeper modeling in this study, it was assumed that the existing pre-stressing force did not decrease. However, the pre-stressing force already decreases in the long term due to factors such as relaxation, creep, and thermal expansion, so in real conditions, pre-stressed sleepers' fatigue life is more affected.
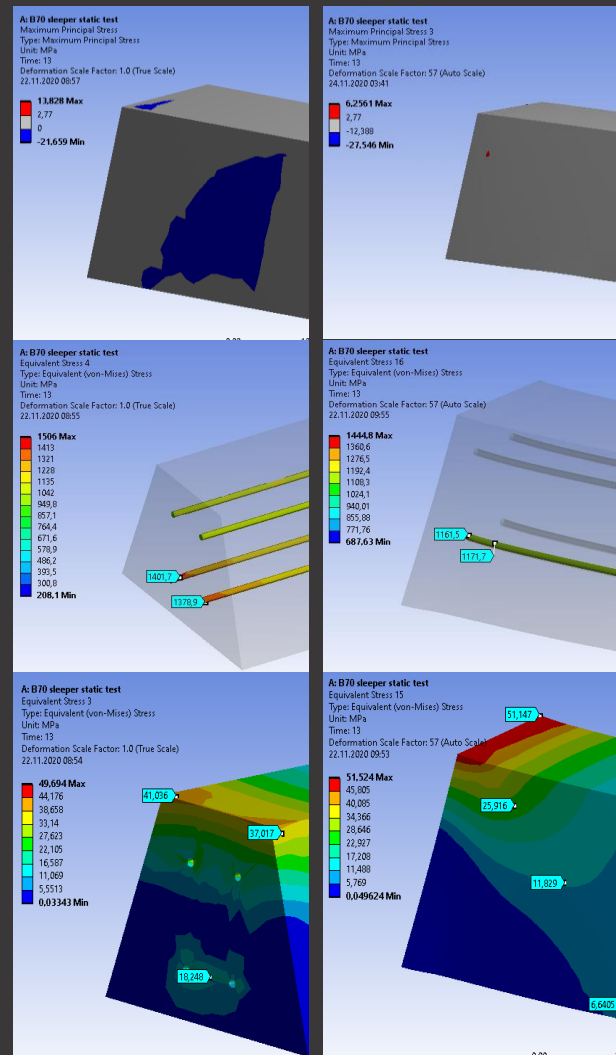

Figure 17. Comparative analysis results of concrete and reinforcements at $Fr_{0.05}$ test loads in N-type sleeper (left-sides) and A-type sleeper (right-sides)

3.2.5. Determination of breaking loads (Fr_B) and development suggestions

The last parameter required in TS EN 13230-2 is the peak load (Fr_B) that the sleeper cannot carry more. Equivalent stress distributions of concrete and reinforcements at this load level are given in Figure 18. For the N-type sleepers, the yielding at reinforcement contact surfaces is reached at 347 kN and the ultimate strength is reached at 375 kN load levels. At a load of 393 kN, the deformations increase so that finite element analysis cannot continue. Afterward, the analysis is terminated automatically by the software since convergence cannot be made. Since the desired information in the standard was reached (peak load value that cannot carry more load), the current analysis was found to be sufficient. In A-type sleepers, reinforcement yield starts at the level of 353 kN test load and rupture does not occur in the reinforcements until the end of the analysis. So, it has been determined that the breaking load of A-type sleepers is 393 kN and can show high deformations. As a matter of fact, in physical tests, the breaking condition of A-type sleepers is reached by crushing the concrete compression lobe. The breaking

loads can be also seen in Figure 15, where concrete equivalent stress development at the bottom of the mid-span cross-section is given. These values are slightly lower than the average breaking load of 430 kN obtained in physical tests. This difference may have resulted from the use of safety coefficients or various assumptions in finite element analyzes. As a result, according to both laboratory experiments and ANSYS finite element analyzes, it was observed that the $Fr_{0.05}$ permanent crack formation load increased significantly as the reinforcement cross-section area increased [1]. At the same time, it is stated that the ultimate strength of sleepers in fatigue tests is higher by using anchored and/or more individual reinforcement [3], and it is shown with the fatigue tests performed on conventional and partially pre-stressed elements with equal final moment capacity, it was observed that the fatigue strength of the partially pre-stressed elements was lower [6]. Therefore, it is considered that reinforcement number and cross-section areas and anchorage geometries, including the non-pre-stressed sleeper production alternative, should be designed taking into account the actual field measurements and reinforcement fatigue limits.

Figure 18. Comparative analysis results of concrete and reinforcements at Fr_B test loads in N-type sleeper (left-sides) and A-type sleeper (right-sides)

4. Conclusion and Discussion

In this study, B70 type pre-stressed concrete sleepers, have been investigated with the positive moment determination tests at the rail seat with progressive failure observations according to EN 13230-2:2016

standard. After tests, detailed cracking, failure, and fatigue analyzes under increasing test loads were performed with ANSYS® finite element analysis results for both types of pre-stressed sleepers. The results obtained through the analysis have been compared with the actual field measurement results, which have become more and more popular in the world in recent years. The findings obtained from the experiments and finite element analyzes are given below;

It was observed that the finite element model and the laboratory test results overlapped substantially. Local stress concentrations can be largely minimized with the ANSYS® SpaceClaim® topology sharing option. On the other hand, pre-stressed concrete sleeper failure stages; The decompression load; The first elastic crack formation load (Fr_r); The first 0.05 mm permanent crack formation load ($Fr_{0.05}$); and the breaking load (Fr_B) values can be accurately predicted with ANSYS® finite element analysis.

In recent years, various field measurement studies have been carried out on railways and the adequacy of the sleeper design loads calculated with empirical approaches in the past has been questioned. Studies in this direction have been encouraged in the postmodern EN 13230-6: 2020 standard. In this study, the results of a recent field measurement were used for sample analysis. Each railway organization should measure the stress, strain, and acceleration data to analyze its road parameters and maintenance status. More realistic results will be obtained as the location variation and measurement time are increased in the measurements to be made.

When the sample field measurement results are examined, it is first seen that impact loads several times higher than the decompression and cracking capacities of pre-stressed concrete railway sleepers occur frequently. But it will not be fully correct to compare field record peak values with the static and fatigue test results of existing sleepers. Because the characteristics of the real railway conditions such as strain rate, load duration, and support conditions are greatly different from the tests in question. However, depending on the railway operating capacity, the number of load repetitions is also quite high, and on the other hand, there are different effects in different parts of the sections and continuous changes in the forced sections. So, the service life begins to decrease due to fatigue.

The fatigue life of pre-stressed sleepers at loads under decompression capacity (for B70 type ~75 kN) is considered to be "infinite" if a correct reinforcement and anchoring mechanism is applied. According to recent field records, over 96% of the loads affecting the sleepers are under decompression capacity.

For the loads above the decompression and below the minimum first crack formation loads (75-150 kN) service life of pre-stressed sleepers begins to decrease due to
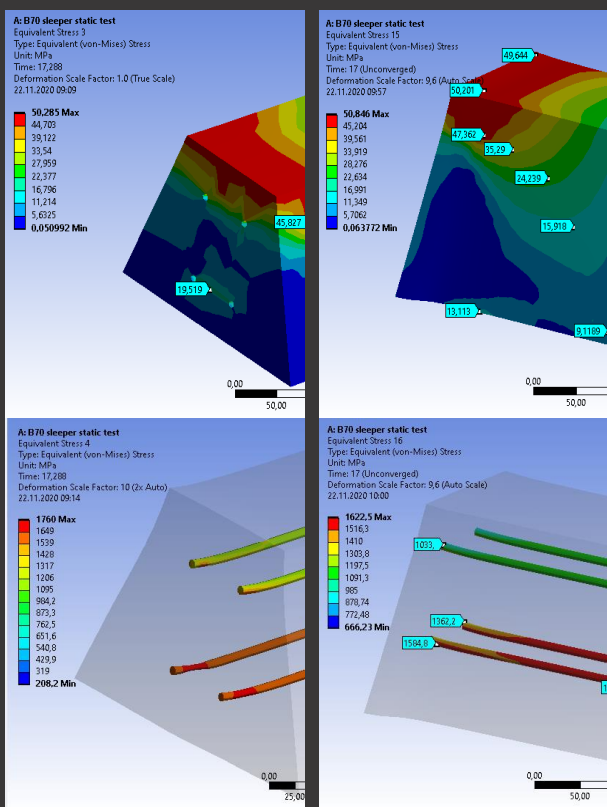
fatigue. According to recent field records, 3.315% of the loads (approximately 10 million) affecting the sleepers are above the decompression capacity. In this region, the stresses in the pre-stressing reinforcement change direction (transforming), and repetitive reversible loads cause early fatigue. According to EN 13230 standard, after 2 million loading cycles, a maximum loss of 45 kN in breaking load is anticipated for B70 type sleepers (from 375 kN to 330 kN).

Loads above the first elastic crack formation load and below the first 0.05 mm plastic crack formation load (150-270 kN), decrease the service life of pre-stressed sleepers relatively faster. According to recent field records, 0.455% of the loads (approximately 1.3 million) affecting the sleepers are above the first elastic cracking load value. It has been determined by laboratory tests that the load value observed in the first crack formation load decreases from 206 kN to 130 kN after a few load repetitions within this region. According to EN 13230 standard, after approximately sixty thousand loads, a maximum loss of 45 kN in breaking load is anticipated for B70 type sleepers (from 375 kN to 330 kN).

Loads above the first 0.05 mm plastic crack formation load and below the breaking load (270-375 kN), decrease the service life of pre-stressed sleepers quite faster. It has been determined by laboratory tests that the load value observed in the first crack formation load decreases from 206 kN to 70 kN after a few load repetitions within this region. According to the recent field records, approximately one thousand loads affecting the sleepers are above the first 0.05 mm plastic cracking load value. According to standards such as EN 13230-1 / 2 on railway sleepers, loads in this region are called exceptional, so a very small number of them are allowed in the service life. With the effect of these cracks, the concrete is damaged, the pre-stress force decreases, and the chlorine ions penetrating the concrete cause corrosion in the pre-stressing steel. Therefore, sleeper life ends before the planned (40/50-year) service life.

A revision of the first crack formation load test is required considering the tensile strength of today's high-performance concrete. Concrete technology in the years when B70 and similar type sleepers were designed, has developed considerably today. The first crack starting load required by the standards or a big part of it can easily be reached in sleepers with high tensile strength of concrete, although not enough pre-stressing force is applied. In this respect, it is thought that it would be more appropriate to control the first crack formation load (Fr_r) value in more detail with the concrete tensile strength used in sleeper production.

According to the first crack formation load (Fr_r), 50% more compression stress occurs in the A-type sleepers compared to N-type sleepers. And at the first 0.05 mm permanent crack formation load ($Fr_{0.05}$), it is seen that 25% higher stresses occur in A-type design than N-type design under $Fr_{0.05}$ load. It is also seen that at this load level in the A-type design, the ultimate strength of 50 MPa has begun to be exceeded both in the compression lobe and near the anchor plate. On the other hand, the number, and width of the cracks are lesser but thicker in an un-ribbed A-type design. Therefore, the ribbed reinforced sleeper design appears to be more advantageous than the non-ribbed anchor plated design in many respects.

In fatigue tests performed on conventional (non-pre-stressed) and partially pre-stressed elements with equal final moment capacity, it was observed that the fatigue strength of the partially pre-stressed elements was lower. Therefore, it is considered that reinforcement number and cross-section areas and anchorage geometries, including the non-pre-stressed sleeper production alternative, should be designed taking into account the actual field measurements and reinforcement fatigue limits.

As a result, the prepared model provides many advantages in matters such as investigating what kind of stress and deformations occur in the background of concrete and reinforcements during the beginning of elastic and plastic cracks in the sleeper and reaching the final strength.

Declaration of Interest Statement

F. Çeçen: Conceptualization, Data curation, Formal analysis, Funding acquisition, Investigation, Methodology, Project administration, Resources, Software, Supervision, Validation, Visualization, Writing – original draft, Writing – review & editing – B. Aktaş: Conceptualization, Data curation, Formal analysis, Funding acquisition, Investigation, Methodology, Project administration, Resources, Software, Supervision, Validation, Visualization, Writing – original draft, Writing – review & editing – B.

Author Contribution Statement

The authors declare that they have no known competing financial interests or personal relationships that could have appeared to influence the work reported in this paper.

References

[1] Çeçen F. & Aktaş B. (2021). New Generation Railway Sleepers and Experimental Research of Domestic FRP Reinforcement Use (in Turkish). Railway Engineering (13), 53-64. https://doi.org/10.47072/demiryolu.803452

[2] Taherinezhad, J., Sofi, M., Mendis, P., & Ngo, T. (2017). Strain rates in prestressed concrete sleepers and effects on cracking loads. *Electronic Journal of Structural Engineering*, *17*, 65-75. https://ejsei.com/EJSE/article/view/220

[3] Derkowski, W., Słyś, B., & Szmit, M. (2014). Effect Of Strands'anchorage System In PC Railway Sleepers On Behaviour Of Its Rail Seat Zone–Experimental Research.. *8th International Conference of AMCM*, 16-18 June, Wroclaw, Poland, 101-108. https://www.infona.pl/resource/bwmeta1.element.bazte ch-86d049c1-10f0-4aa2-bd38-9ad624eb5722

[4] Özcan A. İ., Özden B., Ölçer B. & Gamlı F. D. (2018). Betonarme Traverslerin Gelişimi. *Demiryolu Mühendisliği Dergisi*, 18 (2), 40-44. Available: https://dergipark.org.tr/tr/pub/demiryolu/issue/35609/4 48512

[5] Thürlimann B. (1968). Partially Pre-stressed Members. *International Association for Bridge and Structural Engineering (IABSE) Congress*, 9-14 September, New York, 474-487. http://doi.org/10.5169/seals-8717

[6] The American Concrete Institute-ASCE Committee 423, State-Of-The-Art Report on Partially Pre-stressed Concrete: *ACI 423.5R-99*. http://civilwares.free.fr/ACI/MCP04/4235r_99.pdf

[7] Anonymous, EN 13230-1/2 Standard. 2016. Railway applications, Track, Concrete sleepers and bearers, General requirements/ Pre-stressed Monoblock sleepers. European Committee for Standardization (CEN)

[8] You, R., & Kaewunruen, S. (2019). Evaluation of remaining fatigue life of concrete sleeper based on field loading conditions. *Engineering Failure Analysis*, *105*, 70-86. https://doi.org/10.1016/j.engfailanal.2019.06.086

[9] Çeçen F. (2019). New railway concrete sleeper research about using carbon fiber reinforced polymer rebars with non-pre-stressed and mono-block process, (in Turkish). Master Thesis. Gaziosmanpaşa University. 156s, Tokat. https://www.researchgate.net/publication/344163677

[10] Jokūbaitis, A., Marčiukaitis, G., & Valivonis, J. (2016). Influence of technological and environmental factors on the behaviour of the reinforcement anchorage zone of prestressed concrete sleepers. *Construction and building materials*, *121*, 507-518. http://dx.doi.org/10.1016/j.conbuildmat.2016.06.025

[11] Bezgin N. Ö., (2016). Stresses developed by the vertical forces acting on ballasted railway tracks. *16. Geotechnical Engineering Congress*. 13-14 October. Erzurum, 1-10.

[12] Çelik M. S. (2015). A Multifaced Analysis of Railway Sleepers and Scrutinize of Different Railway Sleepers on An Example Line (in Turkish). Master Thesis. *Istanbul Technical University*. 103s, İstanbul.

[13] Budapest University of Technology and Economics, Department of Applied Mechanics, Index of /~gyebro/files/ans_help_v182. Accessed: 30.10.2020. [Online].https://www.mm.bme.hu/~gyebro/files/ans_hel p_v182/ans_elem/Hlp_E_SOLID186.html

[14] Wolanski A. J. (2004). Flexural behavior of reinforced and pre-stressed concrete beams using finite element analysis. *Marquette University*, Master of Science Thesis, Milwaukee, Wisconsin.

[15] Shayanfar, M. A., Kheyroddin, A., & Mirza, M. S. (1997). Element size effects in nonlinear analysis of reinforced concrete members. *Computers & structures*, *62*(2), 339-352. https://doi.org/10.1016/S0045-7949(96)00007-7

[16] Ovalı İ. (2018). Ansys Workbench. 3. Edition. İstanbul. ISBN 978-605-9118-89-7.

[17] Hammad, M. R. (2015). Non-linear Finite Element Analysis of Reinforced Concrete Beams Strengthened with Carbon Fiber-Reinforced Polymer (CFRP) Technique. *The Islamic University of Gaza*, Civil Engineering Department, Master of Science Thesis, 98s, 2015.

[18] Anonymous, 2002. EN 206-1: Concrete- Part 1: Specification, performance, production and conformity. European Committee for Standardization (CEN)

[19] Anonymous, 2000. TS 500: Requirements for design and construction of reinforced concrete structures. (in Turkish). Turkish Standards Institution, Ankara.

[20] Dalgıç K. D. (2010). Axial Compressive Behaviour And Finite Element Analysis of Low Strength Concrete Confined by Low Modulus Glass Fibre Polymer (in Turkish), Master Thesis. *Istanbul Technical University*. 81s, İstanbul.

[21] Giannakos, K. (2008). Damage of railway sleepers under dynamic loads: a case history from the Greek railway network. Missouri University of Science and Technology, Virginia, 1-11, http://scholarsmine.mst.edu/icchge/6icchge/session08c/ 5